

A New Methodology for Contactless Energy System Using Inductive Coil Positioning Flexibility

Prof. Ms. Madhuri Balasaheb Zambre
(Asst. Prof Department of Electrical
Engineering Modern College of
Engineering,Pune)

Mr. Vivek Vitthal Waiphale
M. Tech(Power System)
Assistant Engineer at
MSEDCL,Maharashtra

Prof. Mr.Chetan Madhukar Gaikwad
(Asst.Professor of E&TC
Department,Sanjeevan Engineering
Technology &Institute,Kolhapur)

Abstract: This paper portrays a system, Contactless transmission of electrical energy from a power source to an electrical load without interconnecting conductor. As of late, expanded remote power exchange frameworks innovation exploration has prompted frameworks with higher effectiveness. Contactless transmission is helpful in situations where interconnecting wires are badly arranged, incomprehensible or perilous. These days electrically worked hardware's are associated with the supply by means of plugs & sockets, however can be hazardous or have constrained life in the vicinity of dampness. In dangerous areas and in submerged applications, the Contactless Energy Transmission System (CETS), by which electrical energy may be transmitted, without electrical association or physical contact, through nonmagnetic media of low conductivity. The CETS has been utilized to exchange up to 5kW over a 10-mm crevice, utilizes high-frequency attractive coupling and empowers module power associations will be made in dangerous natural conditions without the danger of electric shock, short-circuiting, or starting. With contactless Inductive Power Transfer (IPT), it is conceivable to exchange electrical energy to stationary or mobile consumers without contacts, links, or slip rings, another precise and particular configuration displayed in this paper.

INTRODUCTION

Wireless Power transmission uses coupled electromagnetic (EM) fields from an essential subsystem to exchange power through a non-conductive medium. We know The Electromagnetic impelling is relative to the force of the current and voltage in the conductor which delivers the fields. The higher frequency will deliver the more serious the induction effect. Energy is exchanged from a conductor that delivers the fields (Primary) to any conductor on which the fields influence (Secondary). A portion of the energy of the essential conductor passes inductively crosswise over space into secondary conductor and the energy decreases

quickly along the primary conductor. A high frequency current does not go for long separations along a conductor but rather quickly exchanges its energy by induction to neighboring conductors. The higher the frequency more the inductive impacts that exchange energy from circuit to circuit over the space.

Fig. 1 shows a minimum configuration of an IPT system. The electrical energy is transferred through the magnetic field between the coils. The transfer performance can be increased by using high transmission frequencies, alignment of the coils, and special materials like Litz wire and ferrite cores.

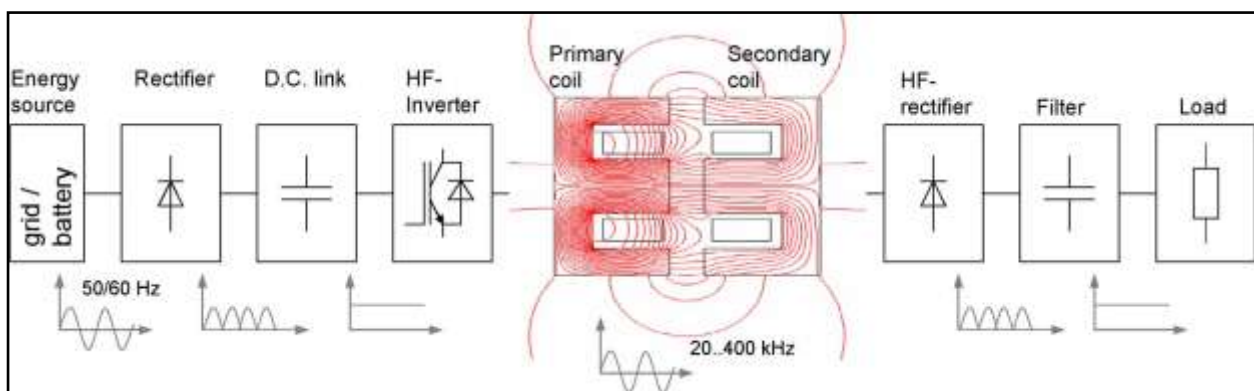


Fig 1: Minimum configuration of a voltage fed inductive power transfer system

In view of the high frequencies, special electronics components are expected to feed the primary coil and to change over the electrical energy on the optional side. The new methodical outline system for the PC helped

configuration had produced for decreasing formative period and the expenses and is proposed in this paper. Along these lines, the power loss of the IPT framework (productivity) and resilience's brought on by mistaken arrangements of the

loops (situating adaptability) or by using so as to stray estimations of electronic gadgets are considered new numerical models and systematic capacities. The models are actualized in another recreation programming apparatus and broke down by an IPT test framework.

The technique proposed in this paper defeats the disadvantages of expense, warm regulation, reaction time, and size by understanding loss mechanism in the transmitter and receiver subsystems. It likewise thinks seriously about how much power is delivered by the receiver subsystem. The fig.1 demonstrates the total inductive power transfer framework which contains magnetic coil and power circuitry for its operation.

1. Basic principle

As depict in Figure 2. It comprises of a transmitter coil L_1 and a receiver coil L_2 . Both coils frame an arrangement of attractively coupled inductors. A rotating current in the transmitter coil produces an attractive field which induces a voltage in the receiver coil. This voltage can be utilized to control a cell phone or charge a battery. The proficiency of the power transfer relies on upon the coupling (k) between the inductors and their quality (Q). The coupling is dictated by the separation between the inductors (z) and the relative size (D_2/D). The coupling is further controlled by the state of the coils and the edge between them.

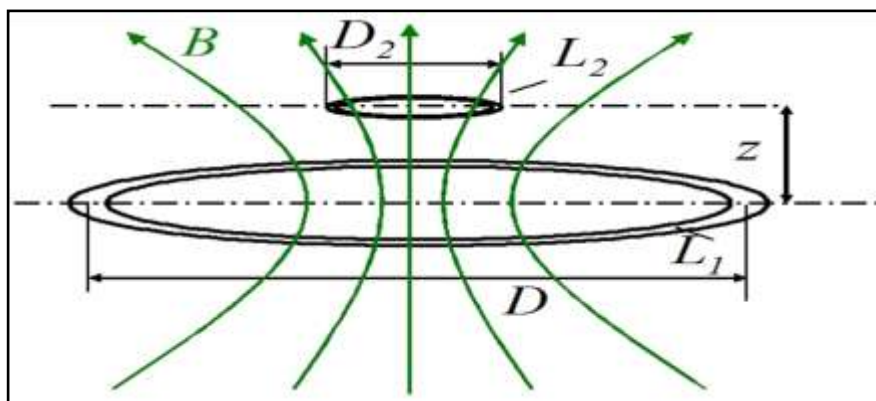


Fig 2: Typical arrangement of an inductively coupled power transfer system

2. Design module of contactless inductive power transfer systems

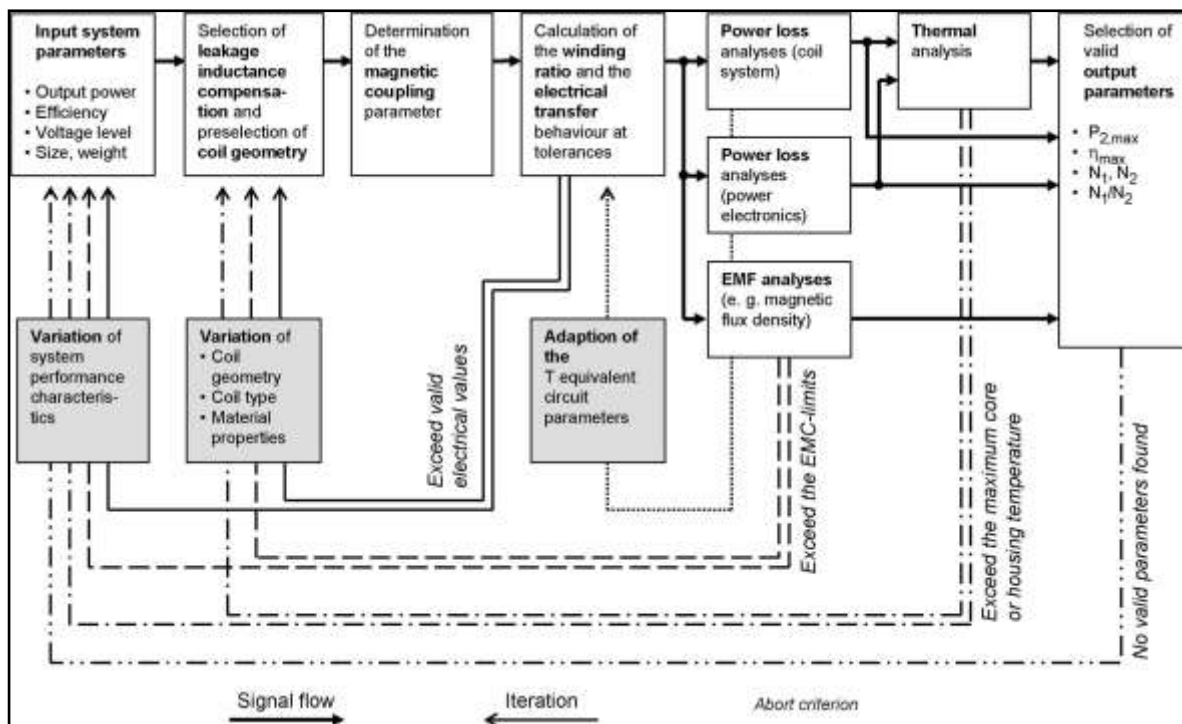


Fig 3: Proposal for solution of a systematic and modular design of contactless inductive power transfer systems

For an efficient IPT system, this work focuses on the magnetic coil system. For the analysis, using the T equivalent circuit is referred, because the main and leakage inductances ($LH, L1\sigma, L2\sigma$) can directly be determined as a result of the FEM simulation [2]. Compared to a conventional transformer LH and $Lx\sigma$ are in the same dimension. At a defined frequency, the power loss of the transformer can be considered by the resistances $R1, R2$, and RFe . The transfer ratio is depicted by $x = N1/N2 \cdot x$. The system parameters (e.g., coil geometry, windings, frequency) have to be determined in compliance with user-defined requirements (performance characteristics), such as voltage and power level, installation size, or costs.

The air gap, straying capacitor values, or coil misalignments can be both required values. After choosing a proper type of leakage inductance compensation strategy, the magnetic coupling parameters ($LH, L1\sigma, L2\sigma$) (Fig. 2) & windings and currents ($N1 \cdot i1, N2 \cdot i2$) can be determined. With the knowledge of $N1 \cdot i1$ and $N2 \cdot i2$, in the next design step, the power loss of the coil system can be determined. Irrespective of EMF, the temperature rise of the system components is another important limiting factor for the transferable power of IPT systems. Thereby, the biological impact, melting temperatures, the thermal stress of power semiconductors, as well as the curie temperature of ferrite cores must be considered. Based on the calculated power loss.

2.1. Design Strategy for Leakage Inductance

The IPT system should be work at high transfer distances and system efficiency. As high transfer distance results in small magnetic coupling therefore to improve efficiency the large leakage inductances must be compensated by capacitors. As shown in (Fig 3 -Step3) this resulting resonance operation which allow the supply of

reactive power. The behavior of resonant transformer is influenced by type of inductance compensation strategy. So resonance capacitance may be placed series or parallel compensation which gives good result.

In step 3(Fig.3) The magnetic coupling parameters is determined based on coil geometry. The transfer power may be increased by increasing input power that is higher flux, by using high frequencies or by resonance operation or by high magnetic coupling. The coil geometry can be defined by the coil diameter 'd' and the transmission distance 'a' is considered.

2.2 Transfer efficiency

Figure 4 demonstrates the ascertained ideal productivity of a framework. All measurements are scaled to the distance across of the bigger coil D, whichever it is (transmitter or receiver loop). The qualities are appeared as a component of the pivotal separation of the loops (z/D). The parameter is the breadth of the smaller coil D2.

The figure demonstrates that

- The proficiency drops drastically at bigger separation ($z/D > 1$) or at an extensive size contrast of the coil ($D2/D < 0.3$)
- A high effectiveness (>90%) can be accomplished at close separation ($z/D < 0.1$) and for loops of comparative size ($D2/D = 0.5..1$)

This demonstrates inductive force transmission over a huge separation, e.g. into a space, is exceptionally wasteful. Today, we can't bear to waste energy for general force applications by utilizing such a framework. Then again, the figure demonstrates that inductive power transmission in premises of the device e.g. at a surface, can be proficient and focused to wired arrangement.

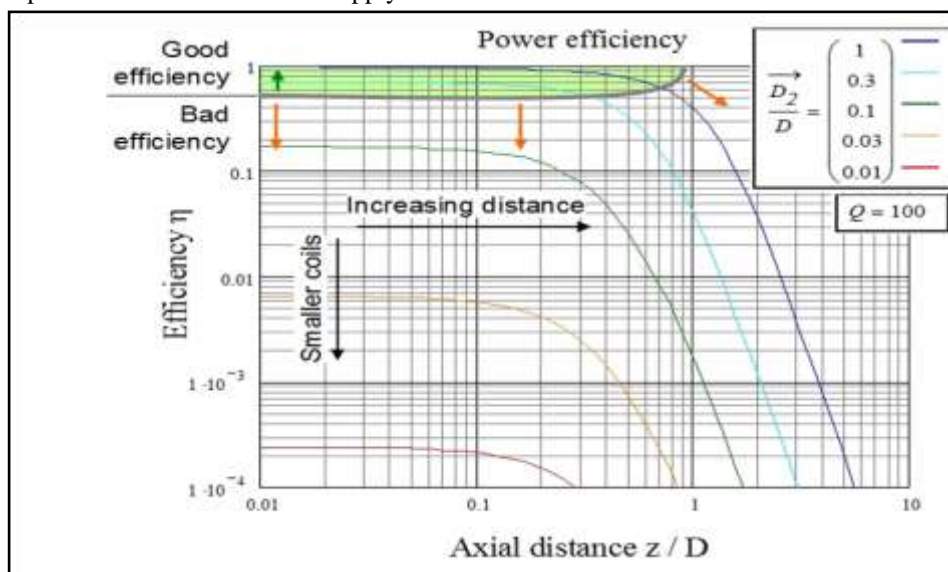


Fig 4: Power efficiency for an inductive power transfer system consisting of loop inductors in dependence on their axis distance z with size ratio as per parameter. Calculated for a quality factor of Q=100.

2.3 Magnetic Coupling Factor

In the event that the collector coil is at a sure separation to the transmitter loop, just a small amount of the magnetic flux, which is created by the transmitter loop, influences the recipient loop and adds to the power transmission. The more flux achieves the receiver; the better the coil are coupled. The evaluation of coupling is done by the coupling element k . The coupling component is a worth somewhere around 0 and 1.1 communicates perfect coupling, i.e. all flux produced enters the recipient coil. 0 communicates a framework, as transmitter and beneficiary coils are autonomous of one another. The coupling variable is dictated by the separation between the inductors and their relative size. It is further controlled by the state of the coils and the edge between them. If coils are axially adjusted, displacement causes decreasing of k . Figure 6 demonstrates this impact for planar coils with 30 mm diameter. It demonstrates the measured and calculated coupling component for parallel coils at diverse misalignment separations at the horizontal axis. Coupling factor in the scope of 0.3 to 0.6.

The definition of the coupling factor is given by:

$$k = \frac{L_{12}}{\sqrt{L_{11} \cdot L_{22}}}$$

It results from the general equation system for coupled inductors:

$$\frac{U_1}{j\omega} = L_{11} \cdot I_1 + L_{12} \cdot I_2$$

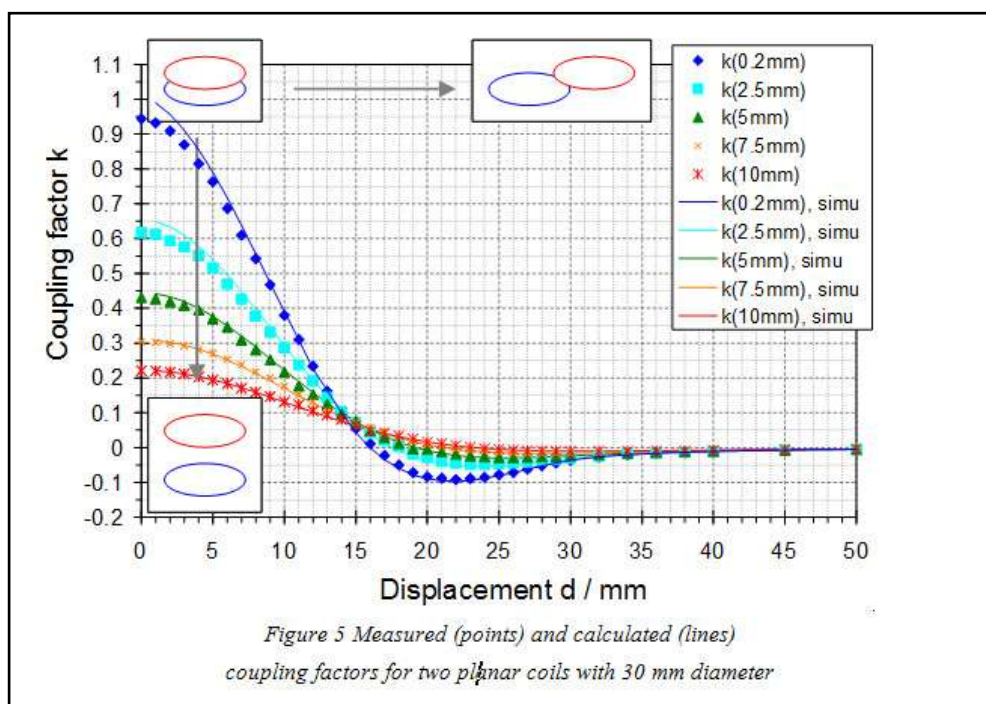
$$\frac{U_2}{j\omega} = L_{12} \cdot I_1 + L_{22} \cdot I_2$$

where U_1 and U_2 are the voltages applied to the coils, I_1 and I_2 are the currents in the coils, L_1 and L_2 are the self-inductances, L_{12} is the coupling inductance and $\omega = 2\pi f$ is the circular frequency.

The coupling factor can be measured at an existing system as relative open loop voltage u :

$$u = \frac{U_2}{U_1} = k \cdot \sqrt{\frac{L_2}{L_1}}$$

If the two coils have the same inductance value, the measured open loop voltage u equals k .



3.0 Electrical Transfer Characteristics at Misalignments:

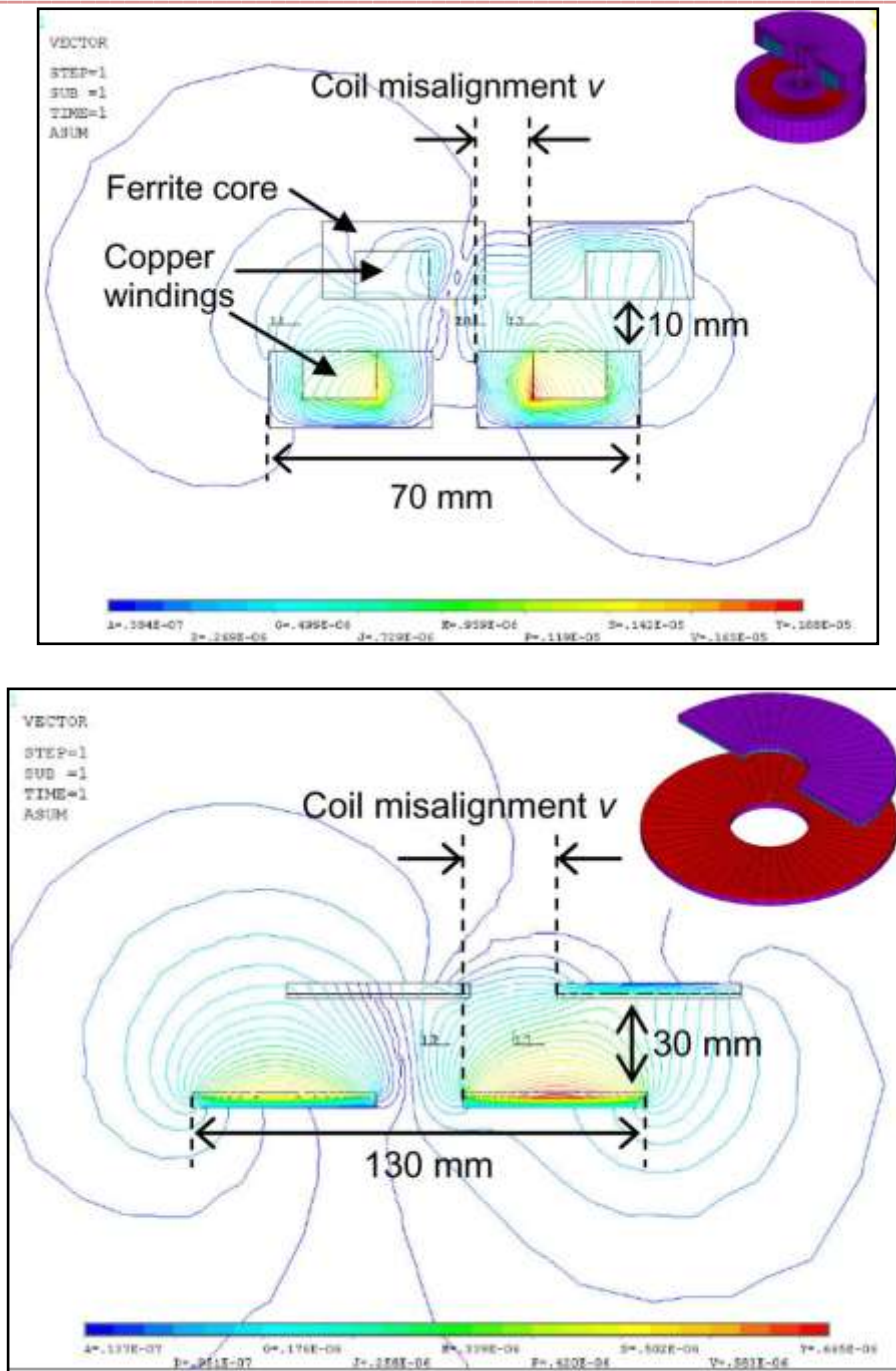


Fig 6: Simulation result (section plane) of the circular coils Pcore70 at a $v = 10$ mm (top) and Flat130 at a $v = 30$ mm (bottom)

Fig 6. shows the calculation and measurement results of the voltage transfer ratio u_2/u_1 of the coil arrangement Pcore70 at a lateral misalignment up to $v = 20$ mm ($C_1 = 52.0$ nF, $C_2 = 41.9$ nF, $N_1 = N_2 = 20$, $fR = 100$ kHz, $R_1 = R_2 = 180$ m Ω , $RL = \{200; 50; 15\}$ Ω corresponds to $QL = \{0.18; 0.72; 2.43\}$). At nominal coil position ($v = 0$), u_2/u_1 is independent of the load QL . At higher misalignment, the voltage transfer ratio u_2/u_1 is very sensitive because of the detuned resonance and depends on both, coil misalignment and load. This is a typical behavior of the series-parallel

resonance operation and occurs in a similar way at variable air gaps or at a variable inverter frequency. A nearly constant ratio of u_2/u_1 at misalignments can be obtained at $QL \approx 1$.

3.1 Maximum power transfer into space

The force that can be taken from a homogeneous attractive field B is subject to the impelled voltage U_{ind} in the utilized recipient coil. Considering it as a circle, for sinusoidal sign shape it results as:

$$U_{ind} = 2\pi f \cdot B \cdot A$$

Where f = frequency and A = loop area.

With the same flux density, a higher force can be transferred at higher frequencies. This implies the result of maximum flux density times the frequency is significant for the power transmission. Utilizing resonance as a part of receiver has been considered. For the actually

frequency range between 100 kHz and 10 MHz the most maximum power is independent of the operating frequency. For frequencies lower than 150 kHz, the maximum power reduces with decreasing frequency. For frequencies above 10 MHz it should be to transmit more power, as per the assumptions.

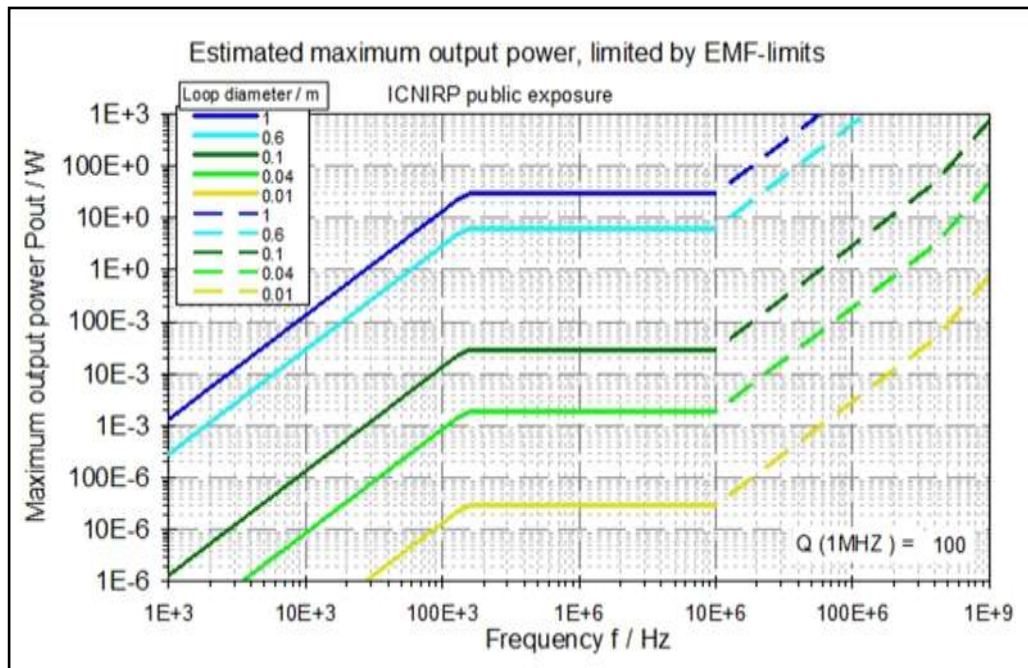


Fig 7: Maximum power reception derived from ICNIRP reference limits for public exposure.

4.0 Test System for Household Appliances

Fig. 8 shows a developed IPT system for the wire and plug less supply of consumer devices on a tabletop. As a result of the proposed design methodology, the coil system was assembled with flat ferrite cores ($d = 130$ mm, $a = 30$ mm, $N_1 = 32$, $N_2 = 16$, Litz wire: $735 \times 71 \mu\text{m}$). The primary power electronics are realized by a voltage fed (dc linked) half-bridge inverter with discrete IGBTs at 100 kHz switching frequency (off-time: 600 ns). On the secondary side, a full-bridge HF-rectifier, a dc link, and an additional inverter are used to allow supplying any dc or ac load (50/60 Hz). The secondary coil, the dc link, and the power electronics, as well as additional control and communication modules, are integrated into the consumer device. The last mentioned modules should ensure a stabilized output voltage and a safe operation (consumer detection and identification). These are very important for nearly all IPT systems used in nonindustrial applications, for example also at e-vehicle charging systems. The IPT system in Fig. 8 is optimized for constant real power (e.g., toaster, kettle, coffee maker, lamps, and electronic devices). The current i_1 is sinusoidal (low harmonics) to enable zero current

switching operation (reduce switching loss and EMI). By using small dc link capacitors on the primary and the secondary side, the load voltage u_L is not constant, but variable (sinusoidal half-waves). As an alternative to [1], [2], in this case, supplying the ac (50/60 Hz) consumer with a half-wave switching matrix converter is possible and favorable [2]. The overall efficiency of the system (incl. feeding inverter, magnetic system, and secondary power electronics) is $\eta = 87. \dots 92\%$, and the output voltage is $u_L = 115$ VRMS ($\pm 10\%$), depending on the alignment of the consumer device (misalignment of the coils). Investigations on the EMF have shown that the magnetic flux density always dominates in the vicinity of the windings (copper wire) and the ferrite layer and falls below the limits at a probe distance from the coils of approximately 10 cm. For human safety, the housing can be used to cover the high flux region. The presented series parallel leakage inductance compensation strategy allows a load-independent voltage transfer ratio and a zero phase angle between the primary current and voltage, which enables a lossless resonant switching operation.

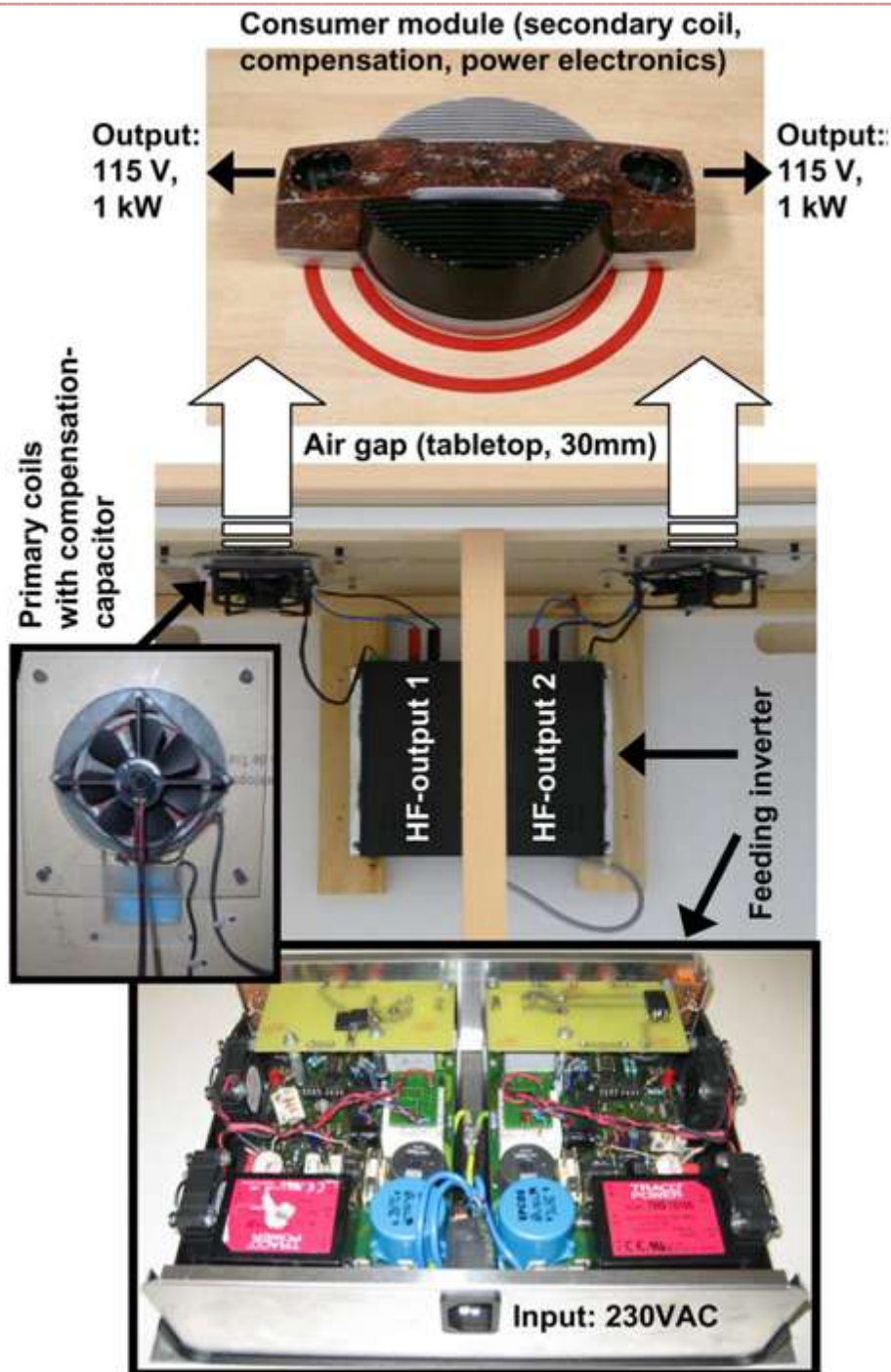


Fig 8: IPT system to supply consumer electronics with high positioning flexibility. The system includes feeding inverter, resonance capacitors, magnetic assembly with flat coils, heat sink module and up to two consumer modules ($2 \times 1 \text{ kW}$), each with double ac output ($1 \times 1 \text{ kW}$ or $2 \times 500 \text{ W}$).

Conclusion and Future Scope:

Wireless power is a lifestyle technology. Like Bluetooth® and Wi-Fi™, As such, it is imperative that a standard application of the technology be introduced to create the greatest opportunity for mass adoption and integration into consumers' lifestyles. The transfer characteristics of IPT systems can be improved by using high frequencies, ferrite

cores, and resonant operation of the coils. This allows the complexity of the system to increase. Therefore, the design of any new IPT system needs at least the consideration of special power loss (efficiency), tolerances (coil positioning flexibility, straying capacitor values), and EMF. Thereby, the most significant aspects of the coil system were modeled by the T equivalent circuit and by the FEM simulation. As an important part of the design methodology, an analytical

expression to find an initial coil geometry for the design and optimization process has been derived. For the computer-aided design, some parts of the methodology were already implemented into a simulation software tool. The proposed design methodology and the developed models are used to develop an IPT system supplying household appliances with an output power of 1 kW per module and at an overall efficiency of 90%. In the next step, models for heat-flow analyses (thermal stress), tolerances, and EMF as well as the proposed iteration (optimization) paths have to be implemented in the software tool. FEM simulation should be necessary to be able to consider no sinusoidal electrical transformer values. Tasks for the extension of the design methodology are the consideration of linear coil geometries, power electronic topologies and devices, and voltage control systems.

In future and not least for the wire and plug-less inductive charging of e-vehicles, the design of an IPT system should also include concepts for a combined inductive energy and data transfer, a bidirectional energy transfer, and for lossless, cost-saving, and lightweight magnetic materials.

References:

- [1] R. Mecke, C. Rathge, W. Fischer, and B. Andonovski, "Analysis of inductive energy transmission systems with large air gap at high frequencies," in *Proc. Eur. Conf. Power Electron. Appl.*, Toulouse, France, 2003, [CDROM].
- [2] R. Mecke, "Contactless inductive energy transmission systems with large air gap," in *Proc. Eur. Conf. Power Electron. Appl.*, Graz, Austria, 2001, [CD-ROM].
- [3] D. Kürschner and C. Rathge, "Contactless energy transmission systems with improved coil positioning flexibility for high power applications," in *Proc. IEEE PESC*, Rhodes, Greece, 2008, pp. 4326–4332.
- [4] D. A. G. Pedder, A. D. Brown, and J. A. Skinner, "A contactless electrical energy transmission system," *IEEE Trans. Ind. Electron.*, vol. 46, no. 1, pp. 23–30, Feb. 1999.
- [5] D. Kürschner, C. Rathge, and A. Hoppe, "Design of inductive power transmission systems considering tolerances and power loss," in *Proc. 35th IEEE IECON*, Porto, Portugal, 2009, pp. 378–383.
- [6] M. L. G. Kissin, J. T. Boys, and G. A. Covic, "Interphase mutual inductance in polyphase inductive power transfer systems," *IEEE Trans. Ind. Electron.*, vol. 56, no. 7, pp. 2393–2400, Jul. 2009.
- [7] J. T. Boys, G. A. Covic, and A. W. Green, "Stability and control of inductively coupled power transfer systems," *IEEE Proc. Elect. Power Appl.*, vol. 147, no. 1, pp. 37–43, 2000.
- [8] K. Chang-Gyun, S. Dong-Hyun, Y. Jung-Sik, P. Jong-Hu, and B. H. Cho, "Design of a contactless battery charger for cellular phone," *IEEE Trans. Ind. Electron.*, vol. 48, no. 6, pp. 1238–1247, 2001.
- [9] G. A. Covic, G. Elliott, O. H. Stielau, R. M. Green, and J. T. Boys, "The design of a contactless energy transfer system for a people mover system," *Proc. Int. Conf. Power Syst. Technol.*, vol. 1, pp. 79–84, 2000.
- [10] T. Hata and T. Ohmae, "Position detection method using induced voltage for battery charge on autonomous electric power supply system for vehicles," *Proc. 8th IEEE Int. Workshop Adv. Motion Control*, pp. 187–191, 2004.
- [11] S. Y. R. Hui and W. W. C. Ho, "A new generation of universal contactless battery charging platform for portable consumer electronic equipment," *IEEE Trans. Power Electron.*, vol. 20, no. 3, pp. 620–627, 2005.
- [12] F. Nakao, Y. Matsuo, M. Kitaoka, and H. Sakamoto, "Ferrite core couplers for inductive chargers," *Proc. Power Convers. Conf.*, pp. 850–854, 2002.
- [13] P. Sergeant and A. Van den Bossche, "Inductive coupler for contactless power transmission," *IET Elect. Power Appl.*, vol. 2, no. 1, pp. 1–7, 2008.
- [14] F. F. A. Van der Pijl, J. A. Ferreira, P. Bauer, and H. Polinder, "Design of an inductive contactless power system for multiple users," *Conf. Rec. IEEE 41st IAS Annu. Meeting*, pp. 1876–1883, 2006.
- [15] W. X. Zhong, L. Xun, and S. Y. R. Hui, "A novel single-layer winding array and receiver coil structure for contactless battery charging systems with free-positioning and localized charging features," *IEEE Trans. Ind. Electron.*, vol. 58, no. 9, pp. 4136–4144, 2011.
- [16] A. J. Moradewicz and M. P. Kazmierkowski, "Contactless energy transfer system with FPGA-controlled resonant converter," *IEEE Trans. Ind. Electron.*, vol. 59, no. 2, pp. 945–951, 2010.
- [17] O. H. Stielau and G. A. Covic, "Design of loosely coupled inductive power transfer systems," *Proc. Conf. Power Syst. Technol.*, vol. 1, pp. 85–90, 2000.
- [18] M. Budhia, G. A. Covic, and J. T. Boys, "Design and optimization of circular magnetic structures for lumped inductive power transfer systems," *IEEE Trans. Power Electron.*, vol. 26, no. 11, pp. 3096–3108, 2011.
- [19] J. Hirai, K. Tae-Woong, and A. Kawamura, "Study on intelligent battery charging using inductive transmission of power and information," *IEEE Trans. Power Electron.*, vol. 15, no. 2, pp. 335–345, 2000.
- [20] M. Budhia, G. Covic, and J. T. Boys, "A new IPT magnetic coupler for electric vehicle charging systems," *Proc. Annu. Conf. IEEE Ind. Electron. Soc.*, pp. 2487–2492, 2010.
- [21] Y. Nagatsuka, N. Ehara, Y. Kaneko, S. Abe, and T. Yasuda, "Compact contactless power transfer system for electric vehicles," *Proc. IPEC*, pp. 807–813, 2010.
- [22] G. Elliott, S. Raabe, G. A. Covic, and J. T. Boys, "Multiphase pickups for large lateral tolerance contactless power-transfer systems," *IEEE Trans. Ind. Electron.*, vol. 57, no. 5, pp. 1590–1598, 2009.
- [23] G. A. Covic, J. T. Boys, M. Budhia, and C.-Y. Huang, "Electric vehicles—Personal transportation for the future," *Proc. World Battery, Hybrid Fuel Cell Elect. Veh. Symp. Exhibi.*, 2010.